

## Near surface composition of some alloys by X-ray photoelectron spectroscopy

M SREEMANY and T B GHOSH\*

Central Glass and Ceramic Research Institute, Jadavpur, Kolkata 700 032, India

\*Department of Physics and Meteorology, Indian Institute of Technology, Kharagpur 721 302, India

\*Corresponding author

MS received 23 March 2001; revised 1 June 2001

**Abstract.** Chemical compositions of the alloys of CuNi ( $\text{Cu}_{0.10}\text{Ni}_{0.90}$ ,  $\text{Cu}_{0.30}\text{Ni}_{0.70}$ ,  $\text{Cu}_{0.70}\text{Ni}_{0.30}$ ) and BiSb ( $\text{Bi}_{0.80}\text{Sb}_{0.20}$ ,  $\text{Bi}_{0.64}\text{Sb}_{0.34}$ ,  $\text{Bi}_{0.55}\text{Sb}_{0.45}$ ) are determined by X-ray photoelectron spectroscopy. The stoichiometries are determined and are compared with the bulk compositions. Possible sources of systematic errors contributing to the results are discussed. Errors arising out of preferential etching in these alloys have been investigated. It has been inferred from such studies that the preferential etching does not enrich the surface composition with a particular component for the two systems reported here. Quantitative results of CuNi system indicate that the surface regions of the  $\text{Cu}_{0.70}\text{Ni}_{0.30}$  alloy is Cu-rich, although no such evidence is observed in case of BiSb system.

**Keywords.** X-ray photoelectron spectroscopy (XPS); near surface composition; alloy.

**PACS Nos** 81.60 B; 79.60; 81.60

### 1. Introduction

Quantitative analysis by photoelectron spectroscopy of binary compounds, particularly of metal alloys is an area, which needs further attention. It has been pointed out that in alloys, surface composition is different from that of the bulk [1–6]. The observed difference has been attributed to surface segregation, preferential sputtering, atomic mixing and radiation-enhanced diffusion imposed by ion cleaning [7]. Although many authors have addressed to these problems [1–6], the potential use of XPS technique to analyse near surface composition of multi-component system remains to be understood.

In this communication, results of quantitative analysis done on CuNi ( $\text{Cu}_{0.10}\text{Ni}_{0.90}$ ,  $\text{Cu}_{0.30}\text{Ni}_{0.70}$ ,  $\text{Cu}_{0.70}\text{Ni}_{0.30}$ ) and BiSb ( $\text{Bi}_{0.80}\text{Sb}_{0.20}$ ,  $\text{Bi}_{0.64}\text{Sb}_{0.36}$ ,  $\text{Bi}_{0.55}\text{Sb}_{0.45}$ ) are presented. Method of linear background subtraction, described elsewhere [8], has been used to measure the intensities of the photoelectron peaks (as areas under the peaks). To determine the stoichiometry, instrumental parameters and the matrix dependent inelastic mean free paths (IMFP) are obtained from literatures. The stoichiometry thus obtained is compared with the chemical composition. Several compositions of CuNi alloy have been selected because CuNi alloy forms a continuous solid solution and have been studied extensively

[1–6]. Compositional results obtained using the technique of linear background subtraction are compared with the reported results. BiSb system has also been selected for quantitative studies. BiSb also forms a complete solid solution over the entire range of compositions.

In order to study the nature of the changes in surface composition of an alloy system due to preferential sputtering, following studies have been made. Different compositions of alloys of CuNi and BiSb are subjected to argon ion sputtering for different instant of times. The corresponding changes in the surface compositions are estimated.

Quantitative results are analysed and possible sources of systematic errors contributing to the results are discussed.

## 2. Composition analysis

For a binary system consisting of species  $A$  and  $B$  of the type  $A_aB_b$ , where  $a$  and  $b$  denote the number of atoms of the species  $A$  and  $B$ , respectively in the multi-component system, the relative mole fraction of the system may be expressed as

$$\frac{X_a}{X_b} = \frac{\sigma_B L_B(\theta) T(E_B) \lambda_M(E_B) I_A}{\sigma_A L_A(\theta) T(E_A) \lambda_M(E_A) I_B}, \quad (1)$$

where,  $\lambda_M(E_A)$  and  $\lambda_M(E_B)$  are the inelastic mean free paths (IMFP) of photoelectrons emerging from the multi-component system corresponding to the energies of the photoelectron lines from species  $A$  and  $B$  respectively.  $I_A$  and  $I_B$  are the corresponding photoelectron line intensities.

### 2.1 Determination of inelastic mean free path $\lambda_M(E)$

IMFPs are determined using various empirical relations available till date [9–11]. Following Penn's algorithm [9] IMFPs can be expressed as

$$\lambda_M(E) = \frac{E}{a_M(\ln E + b_M)}, \quad (2)$$

where,  $a_M$  and  $b_M$  are two parameters characterizing the particular system.

Tanuma *et al* [10] gave the following empirical relation to find the IMFPs,

$$\lambda_M(E) = \frac{E}{E_p^2 \phi [\ln(\tau E)]}. \quad (3)$$

Following Powell [11] ratio of IMFPs for the same solid can be expressed in terms of simple energy dependence as

$$\frac{\lambda_M(E_A)}{\lambda_M(E_B)} = \left( \frac{E_A}{E_B} \right)^{0.7}. \quad (4)$$

In this communication all IMFP calculations are based on relations (2), (3) and (4). Values of  $a_M$ ,  $b_M$ ,  $E_p$ ,  $\phi$ ,  $\tau$  are taken from literatures [9,10].

When matrix dependence of inelastic mean free path is taken into account  $a_M$  and  $b_M$  of relation (2) are modified as follows:

$$\left. \begin{aligned} a_{\text{alloy}} &= Xa_A + (1 - X)a_B \\ b_{\text{alloy}} &= Xb_A + (1 - X)b_B \end{aligned} \right\} \quad (5)$$

where,  $a_A$  and  $b_A$  are the parameters for pure element  $A$  and  $a_B$  and  $b_B$  are that for the element  $B$ ,  $X$  and  $(1 - X)$  are the mole fractions of the elements  $A$  and  $B$  in an alloy of the form  $A_XB_{1-X}$ .

Constants  $E_p$ ,  $\varphi$  and  $\tau$  of relation (3) are also changed when matrix dependence of  $\lambda_M(E)$  is taken into account.

## 2.2 Photoelectron intensity measurements

All the relevant photoelectron line intensities are measured as the areas under the peaks. Areas are obtained assuming the background to be linear [8]. The present method uses the range dependent property of variance of a given distribution.

## 2.3 Ionization cross-section and other instrumental parameters ( $\sigma(h\nu)$ , $L(\theta)$ , $T(E)$ )

To determine the relative atomic concentrations from relation (1), tabulated values of  $\sigma(h\nu)$  [12],  $L(\theta)$  [13] and  $T(E)$  [14] are obtained from literatures.

# 3. Experimental details

## 3.1 Sample preparation

Samples studied are CuNi alloys ( $\text{Cu}_{0.70}\text{Ni}_{0.30}$ ,  $\text{Cu}_{0.30}\text{Ni}_{0.70}$ ,  $\text{Cu}_{0.10}\text{Ni}_{0.90}$ ) and BiSb alloys ( $\text{Bi}_{0.80}\text{Sb}_{0.20}$ ,  $\text{Bi}_{0.64}\text{Sb}_{0.36}$ ,  $\text{Bi}_{0.55}\text{Sb}_{0.45}$ ). CuNi alloys of three known compositions are the product of M/s Johnson and Mathey. The BiSb alloys of different compositions are prepared in the laboratory and the bulk compositions are determined by chemical analysis. All the alloy specimens are polished mechanically before loading into XPS chamber for analysis.

## 3.2 Spectrometer settings

All the spectra recorded here were obtained from VG ESCA LAB MK II, provided with twin anode facility. All the alloy specimens were studied using  $\text{AlK}_\alpha$  (1486.6 eV) unmonochromatized radiation operated at 12 kV and 34 mA. During data acquisition analyser pass energy was maintained at 20 eV for all the narrow scans. Prior to XPS measurements, specimens were cleaned by  $\text{Ar}^+$  sputtering to remove the hydrocarbon contamination. Ion gun was operated at 5 kV and 20  $\mu\text{A}$  with an argon gas pressure of about  $5 \times 10^{-6}$  torr.

## 4. Results and discussions

### 4.1 Studies on CuNi alloy system

Relative mole-fractions ( $X_A/X_B$ ) for CuNi alloys have been determined using relation (1). However, regarding analysis of CuNi alloy, there are contradictory views reported in literatures [1–6] as regard to the surface compositions. Till date literatures in this regard reports both Cu enrichment [2–5] as well as Cu depletion [1,6] near the surface region of this alloy system.

In the year 1976 Wertheim and Hüfner [15] demonstrated that inherent line asymmetry could have an important influence in the determination of alloy composition when the compositions are analysed on the basis of the line intensities of the core line spectra measured from the peak height. They pointed out that the Cu and Ni spectra have different shapes, the Cu spectra having essentially no tail, whereas, the Ni spectra have a very large one. They had shown that in the case of  $\text{Cu}_{0.50}\text{Ni}_{0.50}$  alloy,  $2p_{3/2}$  line intensities (measured in terms of peak heights) of Cu and Ni are very different and that one would come to a very erroneous conclusion by simply taking the ratio of the line intensities. It may be noted here that the cross-sections of Cu  $2p_{3/2}$  and Ni  $2p_{3/2}$  differ by only 13%. Based on these observations, Wertheim and Hüfner [15] suggested that one should calibrate the relative intensities by measuring them in an alloy of known composition. Advanced methods of subtracting the inelastic loss background contribution are now available [16,17]. Tougaard [16] has solved this problem by taking into considerations of all possible physical effects contributing to the losses. Recently Tougaard [18] has worked out the contributions for the background structure arising out of elastic scattering. Besides, there are different empirical methods available to subtract the loss contributions. Among these the most commonly used are linear [8,19] and Shirley type backgrounds [20]. In these methods intensity of a given photoelectron line is measured in terms of the area under a peak.

In the present analysis, intensities of the relevant photoelectron lines are measured from the areas under the peaks. To account for the contributions arising due to instrumental factors (X-ray line width, analyser resolution, life-time of a transition), asymmetric tails due to core-hole conduction electron interactions etc., peak fitting technique described elsewhere [8] have been used. Figures 1a and 1b show the experimental (solid line) profiles of Cu  $2p_{3/2}$  and Ni  $2p_{3/2}$  obtained from  $\text{Cu}_{0.30}\text{Ni}_{0.70}$  alloy. Best-fit profiles (dashed lines) along with the best-fit parameters are also shown in these figures. Difference spectra obtained by subtracting best-fit profile from experimental spectrum are also shown on a horizontal line. To determine the area under a photoelectron peak method of linear background subtraction has been used as has been described by Ghosh and Sreemany [8]. It has been shown that this procedure of background subtraction results to an error of the order of 6% in the intensity measurement.

The errors in quantitative results are influenced by the following factors (with reference to relation (1)):

- (i) cross-section,  $\sigma(h\nu)$
- (ii) instrumental factors ( $L(\theta), T(E)$ )
- (iii) matrix dependent IMFPs ( $\lambda$ )
- (iv) measured values of intensity (inelastic losses, satellite peaks, plasmon losses etc.)

Errors arising out of cross-section (i) and due to experimental geometry (ii) cannot be estimated. However, error due to instrumental parameters is expected to have minimum contribution as Cu  $2p_{3/2}$  and Ni  $2p_{3/2}$  lines are close to each other in energy scale.

IMFP ratios obtained from various empirical relations [9–11] are compared. Table 1 gives results of such calculations for all the compositions studied. It is interesting to note that an excellent agreement among the ratio terms ( $\lambda_{Cu}/\lambda_{Ni}$ ) is obtained using the methods due to Penn [9], Tanuma *et al* [10], and due to Powell [11]. It is evident from such calculations that the matrix dependence of IMFP does not contribute to the quantitative results, as this factor ( $\lambda_{Cu}/\lambda_{Ni}$ ) remains nearly constant (0.913) for all the compositions reported. Hence it may be assumed that the primary source of error in quantitative analysis for multi-component system is due to intensity measurement.

Table 2 gives the results of estimated stoichiometry using relation (1). This table also gives the mole-fraction ratios for three different compositions of CuNi system obtained by using different values of  $\lambda_{Cu}/\lambda_{Ni}$  as given in table 1. The error bar shown against the mole fraction ratios after matrix correction.

**Table 1.** Determined values of inelastic mean free paths for CuNi alloy using various empirical relations.

Alloy system	Profile	Without matrix effect					With matrix effect			
		Penn [9]		Tanuma [10]		Powell [11]	Penn [9]		Tanuma [10]	
		$\lambda_p(E)$	$\frac{\lambda_{Cu}}{\lambda_{Ni}}$	$\lambda_T(E)$	$\frac{\lambda_{Cu}}{\lambda_{Ni}}$	$\frac{\lambda_{Cu}}{\lambda_{Ni}} = \left(\frac{E_{Cu}}{E_{Ni}}\right)^{0.7}$	$\lambda_p(E)$	$\frac{\lambda_{Cu}}{\lambda_{Ni}}$	$\lambda_p(E)$	$\frac{\lambda_{Cu}}{\lambda_{Ni}}$
Cu <sub>0.10</sub> Ni <sub>0.90</sub>	Cu $2p_{3/2}$	7.55	0.916	10.79	1.003	0.910	7.52	0.913	9.89	0.912
	Ni $2p_{3/2}$	8.24		10.75			8.24		10.84	
Cu <sub>0.30</sub> Ni <sub>0.70</sub>	Cu $2p_{3/2}$	7.55	0.916	10.79	1.003	0.910	7.53	0.913	10.06	0.913
	Ni $2p_{3/2}$	8.24		10.75			8.25		11.02	
Cu <sub>0.70</sub> Ni <sub>0.30</sub>	Cu $2p_{3/2}$	7.55	0.916	10.79	1.003	1.910	7.54	0.912	10.49	0.913
	Ni $2p_{3/2}$	8.24		10.75			8.27		11.49	

**Table 2.** Estimated values of mole-fraction ratios for CuNi alloy system using relation (1).

Alloy system	Bulk mole-fraction $\left(\frac{X_{Cu}}{X_{Ni}}\right)_{Bul.}$	Mole-fraction ratio determined using relation (1)				
		Without matrix effect			With matrix effect	
		$\left(\frac{X_{Cu}}{X_{Ni}}\right)_{Penn}$	$\left(\frac{X_{Cu}}{X_{Ni}}\right)_T$	$\left(\frac{X_{Cu}}{X_{Ni}}\right)_{Pow.}$	$\left(\frac{X_{Cu}}{X_{Ni}}\right)_{Penn}$	$\left(\frac{X_{Cu}}{X_{Ni}}\right)_T$
Cu <sub>0.10</sub> Ni <sub>0.90</sub>	0.125	0.114	0.125	0.125	0.125 ± 0.015	0.125 ± 0.015
Cu <sub>0.30</sub> Ni <sub>0.70</sub>	0.428	0.440	0.402	0.443	0.442 ± 0.053	0.442 ± 0.053
Cu <sub>0.70</sub> Ni <sub>0.30</sub>	2.333	2.941	2.688	2.967	2.958 ± 0.355	2.950 ± 0.354

Mole-fraction ratios are being determined using relation (1) for which the values of  $\sigma(h\nu)$  [12],  $\beta$  [13] and  $T(E)$  [14] corresponding to relevant photoelectron lines are taken from published data.

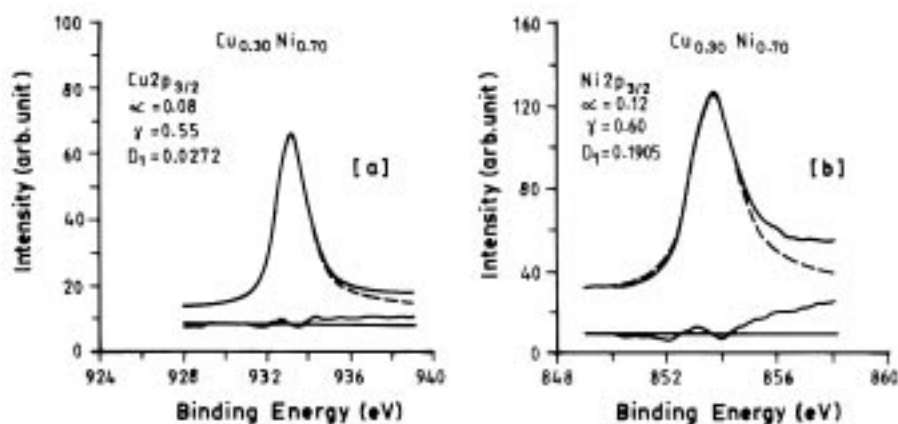


**Figure 1.** Experimentally measured different core-level photoelectron peaks (solid are also line curves) along with their best-fit generated profiles (dashed line curves) from  $\text{Cu}_{0.30}\text{Ni}_{0.70}$ .  $\alpha$ ,  $\gamma$ ,  $D_1$  are the fitting parameters [8]. Residual backgrounds are also shown (solid line curves) over a horizontal level.

Figures 2a–c show some of the core-level photoelectron lines. Solid line curves represent the experimental profiles while dashed lines are the best-fit profiles [8]. Intensity measurements for the relevant lines are done using linear background subtraction [8].

Table 3 gives the ratios of IMFP obtained using various empirical relations [9–11]. This table also gives the matrix corrected values of the IMFPs. As has been observed earlier that the matrix dependence of the ratios of the IMFPs have little effect on the quantitative results for this alloy system.

Table 4 gives the estimated mole-fraction ratios ( $X_{\text{Sb}}/X_{\text{Bi}}$ ) obtained using relation (1) for all the three compositions studied. In order to estimate the uncertainty incorporated in the quantification of alloy due to inelastic mean free path, the mole-fraction ratios are calculated using different values of  $\lambda_{\text{Bi}}/\lambda_{\text{Sb}}$  obtained by various empirical relations. It is interesting to note that the quantitative results obtained using Bi  $4d_{5/2}$  ( $E = 1045.8$ ) and Sb  $3d_{5/2}$  ( $E = 957.9$ ) signals are better than that obtained using Bi  $4f_{7/2}$  ( $E = 1329.4$ ) and Sb  $3d_{5/2}$  signals. This discrepancy may be reasoned as follows: Inelastic mean free path of photoelectrons is a function of energy ( $E$ ). The uncertainty in the ratio of two IMFPs ( $\lambda_1$  and  $\lambda_2$ ) from the same solid corresponding to energies  $E_1$  and  $E_2$  will be less if  $E_1$  and  $E_2$  are not too different [11]. Energy separation is obtained assuming intensity as the only contributing factor. As mentioned above the error in intensity measurement is of the order of 6%. This effectively contributes an error of the order of 12% in the mole-fraction ratios determined. The mole-fraction ratios estimated for the two compositions  $\text{Cu}_{0.10}\text{Ni}_{0.90}$  and  $\text{Cu}_{0.30}\text{Ni}_{0.70}$  lie well within the error bar. Hence no conclusion could be drawn regarding the surface segregation of one of the components. However for 70:30 CuNi the estimated mole-fraction ratio is much larger than the bulk composition. The mismatch (21%) could not be explained in terms of the error in the intensity measurement alone. The other possibility is that the surface composition is different from that of the bulk.

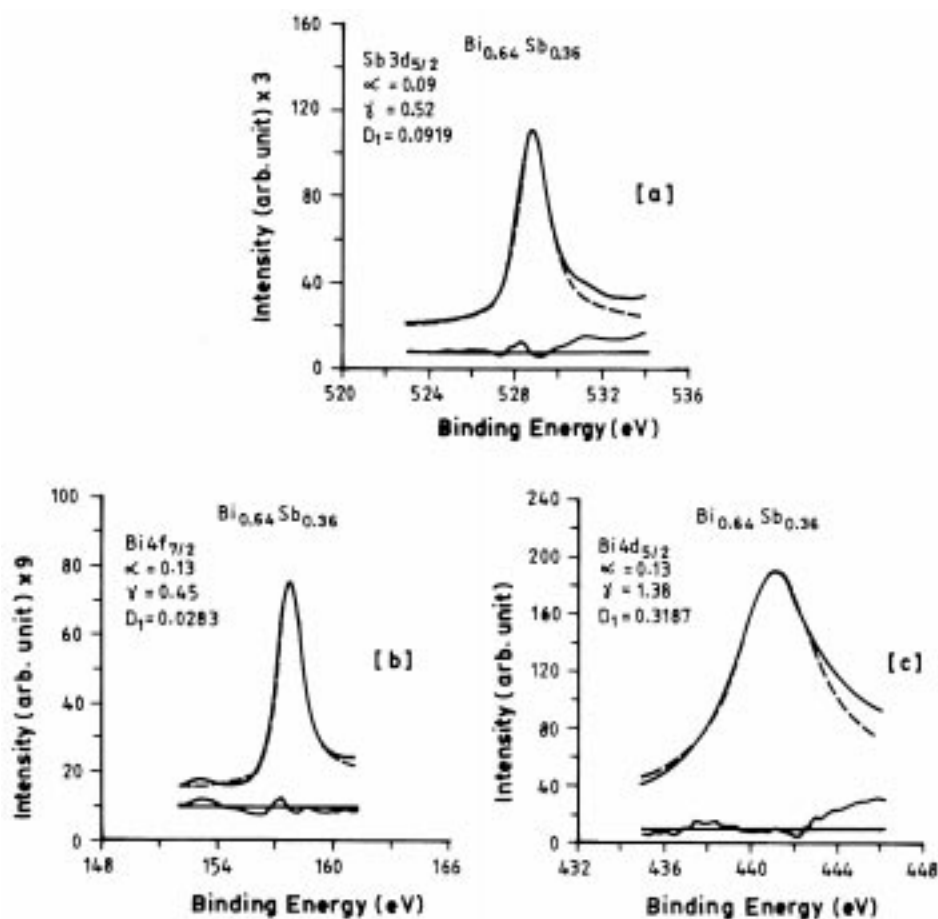


**Figure 2.** Experimentally measured core-level photoelectron spectra (solid line curves) along with their best-fit generated profiles (dashed line curves) from  $\text{Bi}_{0.64}\text{Sb}_{0.36}$ .  $\alpha$ ,  $\gamma$ ,  $D_1$  are the fitting parameters [8]. Residual backgrounds are also shown (solid line curves) over a horizontal level.

It has already been reported that the surface compositions of alloys are different than the bulk compositions [1–6]. The observed difference has been assumed due to surface segregation, preferential etching, atomic mixing etc. In order to determine the composition variation arising out of differential sputter rates, the following studies have been done.

It is reported that the sputter rate of Cu is 1.5 times more than that of Ni [21]. To determine the possible compositional changes near the surface region due to preferential sputtering, sample of  $\text{Cu}_{0.70}\text{Ni}_{0.30}$  was sputtered for different interval of times. For this the etch conditions for subsequent etching were kept constant. Intensities measured in terms of the areas under the photoelectron lines were used to compute the

**Table 3.** Determined values of IMFPs for BiSb system using different empirical relations.

Alloy system	Profile	Without matrix effect					With matrix effect			
		Penn [9]		Tanuma [10]		Powell [11]	Penn [9]		Tanuma [10]	
		$\lambda_p(E)$	$\frac{\lambda_{Bi}}{\lambda_{Sb}}$	$\lambda_T(E)$	$\frac{\lambda_{Bi}}{\lambda_{Sb}}$	$\frac{\lambda_{Bi}}{\lambda_{Sb}} = \left(\frac{E_{Bi}}{E_{Sb}}\right)^{0.7}$	$\lambda_p(E)$	$\frac{\lambda_{Bi}}{\lambda_{Sb}}$	$\lambda_T(E)$	$\frac{\lambda_{Bi}}{\lambda_{Sb}}$
Bi <sub>0.80</sub> Sb <sub>0.20</sub>	Bi 4f <sub>7/2</sub>	21.42	1.299	24.68	1.183	1.285	21.40	1.299	24.92	1.281
	Sb 3d <sub>5/2</sub>	16.49		20.87			16.47		19.45	
Bi <sub>0.64</sub> Sb <sub>0.36</sub>	Bi 4f <sub>7/2</sub>	21.42	1.299	24.68	1.183	1.285	21.42	1.299	25.14	1.281
	Sb 3d <sub>5/2</sub>	16.49		20.87			16.49		19.62	
Bi <sub>0.55</sub> Sb <sub>0.45</sub>	Bi 4f <sub>5/2</sub>	21.42	1.299	24.68	1.183	1.285	21.39	1.299	25.36	1.281
	Sb 3d <sub>5/2</sub>	16.49		20.87			16.47		19.78	
Bi <sub>0.80</sub> Sb <sub>0.20</sub>	Bi 4d <sub>5/2</sub>	17.67	1.072	20.58	0.986	1.063	17.66	1.072	20.76	1.067
	Sb 3d <sub>5/2</sub>	16.49		20.87			16.47		19.45	
Bi <sub>0.64</sub> Sb <sub>0.36</sub>	Bi 4d <sub>5/2</sub>	17.67	1.072	20.58	0.986	1.063	17.86	1.072	20.95	1.068
	Sb 3d <sub>5/2</sub>	16.49		20.87			16.49		19.62	
Bi <sub>0.55</sub> Sb <sub>0.45</sub>	Bi 4d <sub>5/2</sub>	17.67	1.072	20.58	0.986	1.063	17.66	1.072	21.13	1.068
	Sb 3d <sub>5/2</sub>	16.49		20.87			16.47		19.78	

**Table 4.** Estimated mole-fraction values for BiSb using relation (1).

Alloy system	Bulk mole-fraction $\left(\frac{X_{Sb}}{X_{Bi}}\right)_{Bul.}$	Mole-fraction ratio determined using relation (1)				
		Without matrix effect			With matrix effect	
		$\left(\frac{X_{Sb}}{X_{Bi}}\right)_{Penn}$	$\left(\frac{X_{Sb}}{X_{Bi}}\right)_T$	$\left(\frac{X_{Sb}}{X_{Bi}}\right)_{Pow.}$	$\left(\frac{X_{Sb}}{X_{Bi}}\right)_{Penn}$	$\left(\frac{X_{Sb}}{X_{Bi}}\right)_T$
Bi <sub>0.80</sub> Sb <sub>0.20</sub>	0.250	0.263 <sup>a</sup>	0.240 <sup>a</sup>	0.255 <sup>a</sup>	0.263 <sup>a</sup> ± 0.032	0.260 <sup>a</sup> ± 0.031
		0.233 <sup>b</sup>	0.214 <sup>b</sup>	0.231 <sup>b</sup>	0.233 <sup>b</sup> ± 0.028	0.232 <sup>b</sup> ± 0.028
Cu <sub>0.30</sub> Ni <sub>0.70</sub>	0.562	0.543 <sup>a</sup>	0.494 <sup>a</sup>	0.526 <sup>a</sup>	0.543 <sup>a</sup> ± 0.065	0.535 <sup>a</sup> ± 0.064
		0.563 <sup>b</sup>	0.518 <sup>b</sup>	0.558 <sup>b</sup>	0.563 <sup>b</sup> ± 0.068	0.561 <sup>b</sup> ± 0.067
Cu <sub>0.70</sub> Ni <sub>0.30</sub>	0.818	1.101 <sup>a</sup>	1.003 <sup>a</sup>	1.067 <sup>a</sup>	1.101 <sup>a</sup> ± 0.132	1.087 <sup>a</sup> ± 0.130
		0.961 <sup>b</sup>	0.884 <sup>b</sup>	0.953 <sup>b</sup>	0.961 <sup>b</sup> ± 0.115	0.957 <sup>b</sup> ± 0.115

<sup>a</sup>Determined using Bi 4f<sub>7/2</sub> and Sb 3d<sub>5/2</sub> signals.

<sup>b</sup>Determined using Bi 4d<sub>5/2</sub> and Sb 3d<sub>5/2</sub> signals.

Mole-fraction ratios are being determined using relation (1) for which the values of  $\sigma(h\nu)$  [12],  $\beta$  [13] and  $T(E)$  [14] corresponding to relevant photoelectron lines are taken from published data.

mole-fractions from relation (1). Figure 3 describes the results of such studies where estimated mole-fraction ratio of Ni to Cu is plotted against etch times. In this figure dashed horizontal line represents the bulk composition (in terms of the mole-fraction ratio) of the alloy. A scatter of the order of 2–11% about the mean value is observed. This study clearly indicates that surface composition of the said alloy does not change due to preferential etching. It is worthwhile to mention that even if there are changes in the surface

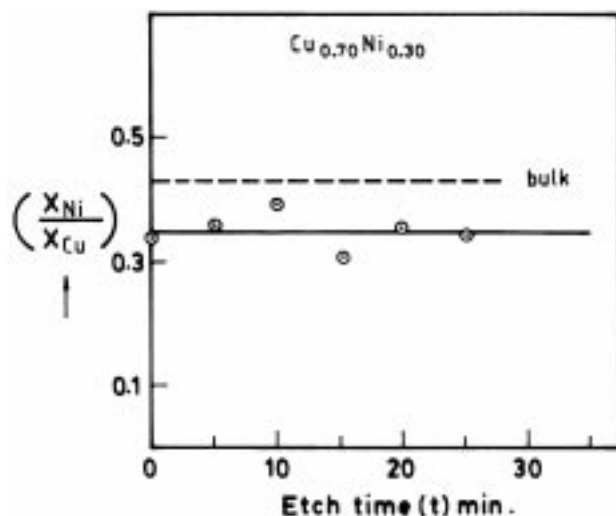


**Figure 3.** Variation of mole-fraction ratio of Ni to Cu with Ar<sup>+</sup> sputter time for Cu<sub>0.70</sub>Ni<sub>0.30</sub>. Dashed line represents the bulk mole-fraction.

compositions, it could not be inferred by the present approach. This is because the scatter in the values in the mole-fraction lies well within the error in estimated mole-fraction ratio ( $\sim 12\%$ ).

It is interesting to note that the mean atomic ratio ( $X_{\text{Ni}}/X_{\text{Cu}}$ ) as measured experimentally from XPS peak area is 0.35 (figure 3), which is lower than that of the bulk (0.428). From this it could be inferred that the surface region of Cu<sub>0.70</sub>Ni<sub>0.30</sub> alloy is copper-rich region. This observation is in confirmation with earlier findings. Using the present method of intensity measurement (from areas under the peaks), no conclusive evidence regarding surface segregation for lower concentrations of the CuNi alloy (30:70,10:90) could be made. However, Webber *et al* [3] studied segregation of Cu on different crystalline faces of CuNi single crystals. They had shown some crystallographic planes of Cu<sub>5</sub>Ni<sub>95</sub> are Cu rich. They had compared the segregations on {210} and {111}, and had shown segregation on {210} is more than {111}. They have attributed this due to the surface roughness of the {210} planes. Following Weber *et al* and others [2–5], it could be inferred from the above study that the observed higher value of the mole fraction ratio ( $X_{\text{Cu}}/X_{\text{Ni}}$ ) 2.950 is due to surface segregation of Cu atoms in 70:30 CuNi alloy.

Table 5 gives the quantitative results obtained following Wertheim and Hüfner [15]. Cu<sub>0.70</sub>Ni<sub>0.30</sub> is taken as the standard to calibrate the intensity scale. There is an anomaly in the compositions when compared with the results of table 2. This anomaly could be interpreted as due to the error involved in normalizing the intensity scale. In the present analysis it had been shown earlier that the surface region of 70:30 CuNi alloy is Cu-rich region, hence assuming its composition as the bulk composition (70:30) leads to wrong value of the normalization factor. From relation 1 it could be written for a pair of photoelectron lines,

$$I_{\text{Cu}}/I_{\text{Ni}} = C \cdot (X_{\text{Cu}}/X_{\text{Ni}}).$$

**Table 5.** Compositions obtained for CuNi alloys following calibration method due to Wertheim and Hüfner [15].

Alloy studied	Calibration constant ( $C$ )	Bulk mole-fraction ratio ( $X_{\text{Cu}}/X_{\text{Ni}}$ )	After calibration		
			$X_{\text{Cu}}$	$X_{\text{Ni}}$	$\left(\frac{X_{\text{Cu}}}{X_{\text{Ni}}}\right)_{\text{calib.}}$
$\text{Cu}_{0.10}\text{Ni}_{0.90}$	1.408	0.111	0.09	0.91	0.099
$\text{Cu}_{0.30}\text{Ni}_{0.70}$		0.428	0.26	0.74	0.351

Quantitative results obtained using  $\text{Cu}_{0.70}\text{Ni}_{0.30}$  as calibrating sample.

**Table 6.** Compositions obtained for BiSb system following calibration method under ref. [15].

Alloy studied	Calibration constant ( $C$ )	Bulk mole-fraction ratio ( $X_{\text{Sb}}/X_{\text{Bi}}$ )	After calibration		
			$X_{\text{Sb}}$	$X_{\text{Bi}}$	$\left(\frac{X_{\text{Sb}}}{X_{\text{Bi}}}\right)_{\text{calib.}}$
$\text{Bi}_{0.80}\text{Sb}_{0.20}$	0.995	0.250	0.24	0.786	0.272
$\text{Bi}_{0.55}\text{Sb}_{0.45}$		0.818	0.533	0.467	1.141

Quantitative results obtained using  $\text{Bi}_{0.64}\text{Sb}_{0.36}$  as calibrating sample and Bi  $4f_{7/2}$  and Sb  $3d_{5/2}$  signals are considered.

Using relation (1) the sensitivity factor ( $C$ ) is obtained as 1.040. Table 2 compositions are calculated using this value of the sensitivity factor. However, following Wertheim and Hüfner [15] this value is 1.408 (table 5).

#### 4.2 Studies on BiSb alloy system

Different compositions of BiSb alloys prepared have been studied by XPS. Quantitative estimations obtained using XPS techniques is compared with the bulk compositions between Bi  $4d_{5/2}$  and Sb  $3d_{5/2}$  is less compared to Bi  $4f_{7/2}$  and Sb  $3d_{5/2}$ . Hence the uncertainty in the ratio of IMFPs in the first case is less compared to second case. Finally, considering that the present method of intensity measurement adds an uncertainty of the order of 6%, the agreement achieved in the determined mole-fraction ratio with respect to that of the bulk for different compositions of BiSb alloys except  $\text{Bi}_{0.55}\text{Sb}_{0.45}$  is quite excellent.

Table 6 gives the quantitative results for  $\text{Bi}_{0.80}\text{Sb}_{0.20}$  and  $\text{Bi}_{0.55}\text{Sb}_{0.45}$  alloys following calibration method due to Wertheim and Hüfner [15]. Here intensity scale is calibrated against  $\text{Bi}_{0.64}\text{Sb}_{0.36}$  alloy. A significant difference between the determined mole-fraction ratios and the bulk compositions is observed.

As discussed earlier, possible sources of error for the observed mismatch may arise either due to (i) intensity measurements or (ii) may arise due to preferential sputtering or may be due to both.

Etching for different intervals of time has been carried out keeping etching conditions identical. After each etching the XPS compositional analysis has been done. Figure 4 describes the results of such studies. Scattering in the estimated values of mole-fraction

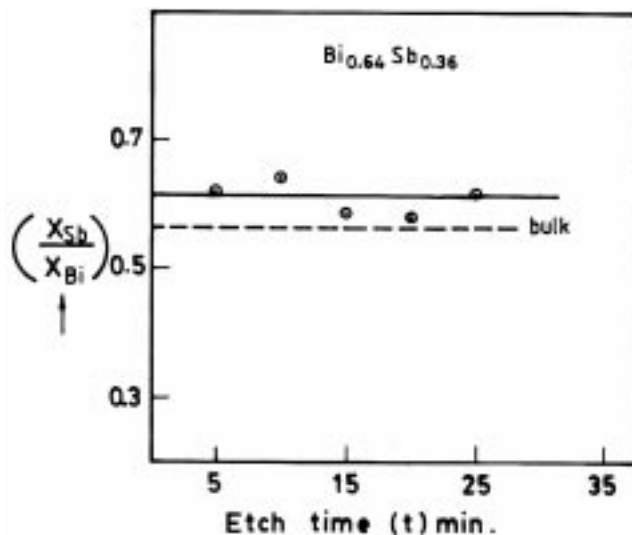


**Figure 4.** Variation of mole-fraction ratio of Sb to Bi with  $\text{Ar}^+$  sputter time for  $\text{Bi}_{0.64}\text{Sb}_{0.36}$ . Dashed line represents the bulk mole-fraction.

ratio ( $X_{\text{Sb}}/X_{\text{Bi}}$ ) at different intervals of etching is observed. The observed scattering is within 6% with respect to the mean value (0.615). This nature of compositional variation with the extent of etching clearly suggests that preferential sputtering does not contribute to the error in the quantitative results. Even if it has any contribution it is well within the error of the present method of intensity measurement.

## 5. Conclusions

Primary sources of error in quantitative estimation of the alloy systems (CuNi, SbBi) have been identified.

Matrix dependence of IMFP is found to have little contribution to the quantitative results. Energy dependence of instrumental parameters is found to have negligible contributions provided the pair of photoelectron lines lies close in energy scale.

Errors in estimated composition, arising out of preferential etching in multi-component system have been investigated. Compositional analysis is done on samples of the alloys for different extent of etching. The results of such study have shown a scatter in the mole-fraction ratios around a mean value. It has been inferred from such studies that the preferential etching does not enrich the surface composition with a particular component. Calibration method proposed by Wertheim and Hüfner [15] has been used to determine the compositions of the alloy systems studied. It has been shown that the process of normalizing the intensity scale may lead to wrong quantitative results if the surface composition is different from the bulk.

Studies on CuNi system have indicated that the surface region of 70:30 CuNi is Cu-rich. Advanced technique of intensity measurement is expected to yield better information regarding surface composition at lower Cu-concentrations.

## References

- [1] T Koshikawa, K Gota, N Saeki, R Shimizu and E Sugata, *Surf. Sci.* **79**, 461 (1979)
- [2] C R Brundle and K Wandelt, *J. Vac. Sci. Technol.* **18**, 537 (1981)
- [3] P R Weber, M A Morris and Z G Zhang, *J. Phys.* **F16**, 413 (1986)
- [4] U Vahalia, P Dowben and A Miller, *J. Vac. Sci. Technol.* **A4**, 1675 (1986)
- [5] V Miteva, D Karpuzov, P Ivanov and Sangelova, *Nucl. Instrum. Methods Phys. Res.* **B85**, 340 (1994)
- [6] S Tougaard and C Jansson, *Surf. Interface Anal.* **20**, 1013, (1993)
- [7] P Sigmund, *Sputtering by ion bombardment* edited by R Berisch, Topics in Applied Physics, (Springer, Berlin, 1981) vol. 47, pp. 9
- [8] T B Ghosh and M Sreemany, *Appl. Surf. Sci.* **64**, 59 (1993)
- [9] D R Penn, *J. Electron Spectrosc. Rel. Phenom.* **9**, 29 (1976)
- [10] S Tanuma, C J Powell and D R Penn, *Surf. Interface Anal.* **11**, 577 (1976)
- [11] C J Powell, *J. Vac. Sci. Technol.* **A3**, 1338 (1985)
- [12] J H Scofield, *J. Electron Spectrosc. Rel. Phenom.* **8**, 129 (1976)
- [13] R F Railman, A Msezane and S T Manson, *J. Electron Spectrosc. Rel. Phenom.* **8**, 389 (1976)
- [14] A E Hughes and C C Phillips, *Surf. Interface Anal.* **4**, 220, (1982)
- [15] G K Wertheim and S Hüfner, *J. Inorg. Nucl. Chem.* **38**, 1701 (1976)
- [16] S Tougaard, *Surf. Interface Anal.* **11**, 453 (1988)
- [17] J E Castle, H Chapman-Kpodo, A Proctor and A M Salvi, *J. Electron Spectro. and Rel. Phenom.* **106**, 65 (2000)
- [18] A Dubus, A Jablonski and S Tougaard, *Prog. Surf. Sci.* **63**, 135 (2000)
- [19] C J Powell and P E Larson, *Appl. Surf. Sci.* **1**, 186 (1978)
- [20] D A Shirley, *Phys. Rev.* **B5**, 4709 (1972)
- [21] V G Scientific operating instructions for ESCA LAB MK II, Ch. 4 (literature for Ag21 ion source) pp. 29